

Thermomechanical Creep Fatigue Life Time Comparison in Three Heat-Resistant Steels

P. Wang¹, L. Cui², A. Scholz, S. Linn and M. Oechsner

¹ Institut für Werkstoffkunde (IfW), Technische Universität Darmstadt, Grafenstrasse 2, 64283 Darmstadt, Germany, E-mail address: pwang@mpa-ifw.tu-darmstadt.de

² IfW Darmstadt, since July 2011 School of Mechanical Engineering, Xi'an Shiyou University, Dianzi Erlu 18, 710065 Xi'an, Shaanxi, China

ABSTRACT. *Steels with various chromium contents are widely applied in steam turbine components and have been introduced steadily in the last decades. The initial aim in the development of such steels is to achieve high performance in creep resistance. Due to the fluctuations of electrical power demand nowadays, power plants are increasingly forced to run at varying utilization levels, which can shift the critical load to fatigue domain by superimposed creep on the heated surface of components. In the current paper, the creep fatigue behavior of 1%-, 2%- and 10%Cr steels under multiaxial loading is described. The experimental investigation was conducted on steels of the types 1Cr-1Mo-Ni-V, 2Cr-1Mo-W-V and 10Cr-1Mo-1W-V-Nb-N as representative samples for each of the three steel grades. The experimental database consists of uniaxial as well as biaxial creep fatigue experiments which were conducted on a biaxial cruciform testing machine. Of special interest was a lifetime comparison of experiments under thermomechanical and isothermal loading at the maximum application temperature. A unified viscoplastic constitutive material model with an incorporated damage variable was applied for lifetime assessment. Finally, metallographic investigations contribute to a better knowledge of the evolution of damage and its modelling. The investigation shows slightly different effects on lifetime, dependent on the three steel grades.*

INTRODUCTION

Due to the need for flexibility in satisfying electrical power demand nowadays, coal-fired power plants are increasingly forced to run at varying utilization levels. The temperature transients during startup and shutdown cause strain cycling with variable thermal stresses on the heated surfaces of turbine components. In steam turbines, turbine shafts belong to the most safety related components, and thus particular attention should be paid to the lifetime assessment. Steels with various chromium contents are applied for the manufacturing of steam turbine shafts and have been improved constantly in the last decades. The experimental investigation of this paper

was conducted for steels of the types 1Cr-1Mo-Ni-V (German grade 28CrMoNiV4-9), 2Cr-1Mo-W-V (German grade 23CrMoNiWV8-8) and 10Cr-1Mo-1W-V-Nb (German grade X12CrMoWVNbN10-1-1) as representatives for each of the three steel grades.

The forged steel 28CrMoNiV4-9 belongs to the class of 1%Cr steels which have been used for steam turbine components in fossil power plants (plants operating at >22MPa at 538 to 565°C) since the 1960s. In addition to exhibiting decreasing mechanical strength with increasing temperature, the material provides insufficient corrosion resistance at temperatures higher than 550°C because of the relatively low chromium content. The heat resistant steel 23CrMoNiWV8-8 was originally developed for the production of steam turbine shafts from one-piece, so-called monoblock shafts. Due to a low thermal expansion coefficient and sufficient thermal conductivity, the investigated steel is suitable for larger forging pieces. The material reaches its limits when constructively higher strengths than the yield strength are necessary or the operating temperature is above 565°C. In modern supercritical fossil power plants (main steam temperatures of 580 to 600°C and pressures of 24 to 35MPa), modern 9-12%Cr ferritic-martensitic steels are applied. The investigated 10%Cr steel of the type X12CrMoWVNbN10-1-1 was developed in European COST Material Programs [1]. It is used for rotor shafts which are designed for operating temperatures up to 600°C.

The initial aim in the development of such steels is primarily to improve their high performance in creep resistance. The variable loading conditions can shift the critical load to the fatigue domain by superimposed creep on the heated surface of components. In the current paper, the creep fatigue behavior of the three steels under multiaxial and thermomechanical fatigue (TMF) loading was investigated.

EXPERIMENTAL

Uniaxial experiments were conducted on cylindrical specimens. They were performed on a servo-hydraulic testing machine. Total strain was controlled by the use of a side contact extensometer. Additionally, biaxial experiments were performed on a biaxial cruciform testing system [2]. The cruciform specimen (Fig. 1) was designed by finite element analysis (FEA) in order to achieve a uniform stress distribution in the gauge section. Total strain control was performed by the use of a cruciform side contact biaxial extensometer. Details of specimens and experimental setup are given in [2].

The testing program contains “service-type” [3] and “service-like” [4] experiments. The strain controlled service-type loading cycle with four hold times is illustrated in Fig.2a and Fig. 2b. It is characterized by a compressive strain hold phase 1 simulating start-up conditions, a zero strain hold phase 2 approximating temperature equilibrium during constant loading, a tensile strain hold phase 3 simulating shut-down conditions and an additional zero strain hold phase 4 which characterizes zero loading condition. A multi-stage service-type cycle is formed by a sequence of service-type loading cycles which represent cold, warm and hot starts of steam turbines [3]. The strain and stress curves of a service-like loading cycle (Fig. 2c and 2d) are based on elastic-plastic FEA

for the area of a rotor slot in the inlet of a high pressure rotor for the typical temperature profiles of cold, warm and hot starts.

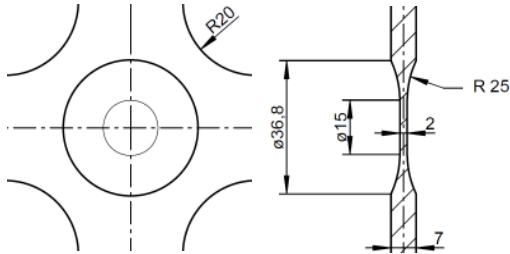


Figure 1. Cruciform specimen used for biaxial creep fatigue experiments.

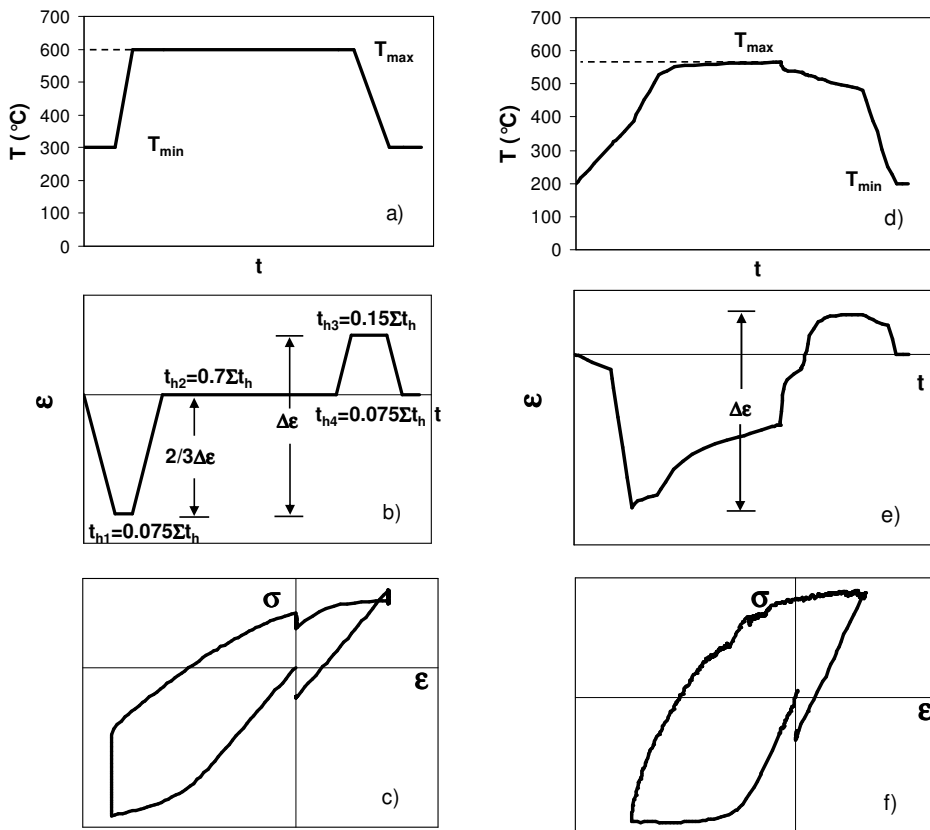


Figure 2. Single-stage service-type [3][5] temperature cycle (a), strain cycle (b) and corresponding hysteresis loop (c), service-like [9][12] temperature cycle (d), strain cycle (e) and corresponding hysteresis loop (f), both representing cold start cycle, sum of hold times $\Sigma t_h = t_{h1} + t_{h2} + t_{h3} + t_{h4}$. For more details refer to [3][5][9][12].

LIFE TIME COMPARISON

The numbers of cycles to crack initiation in relationship to mechanical strain range are summarized in Fig. 3. The axial strain ranges $\Delta \epsilon_x$ in the direction x were applied to characterize the biaxial experiments. In the case of three-stage service-type experiments the values of hot start strain ranges were applied to characterize lifetime. The TMF

service-type lives are compared with isothermal service-type life values (dashed line) and isothermal push-pull fatigue life line (solid line) for the steels X12CrMoWVNbN10-1-1 and 28CrMoNiV4-9. For 23CrMoNiWV8-8, the TMF service-like life values are compared with isothermal service-like lives (dashed line) and isothermal push-pull fatigue life line (solid line) at the maximum temperature. It can be observed that both isothermal service-type (Fig. 3a) and isothermal service-like (Fig. 3b) life values are shorter than the corresponding push-pull fatigue life values at the same strain range.

For the modern 10%Cr-steel (Fig. 3a) the service-type TMF life values are significantly shorter than isothermal life values. But in the case of 23CrMoNiWV8-8 the TMF life values are approximately in the same order of magnitude compared to isothermal life values (Fig. 3b). A different observation has been made in the case of the steel with the lowest chromium content, steel 28CrMoNiV4-9 (Fig. 3c). Here TMF life values are significantly higher than isothermal life values.

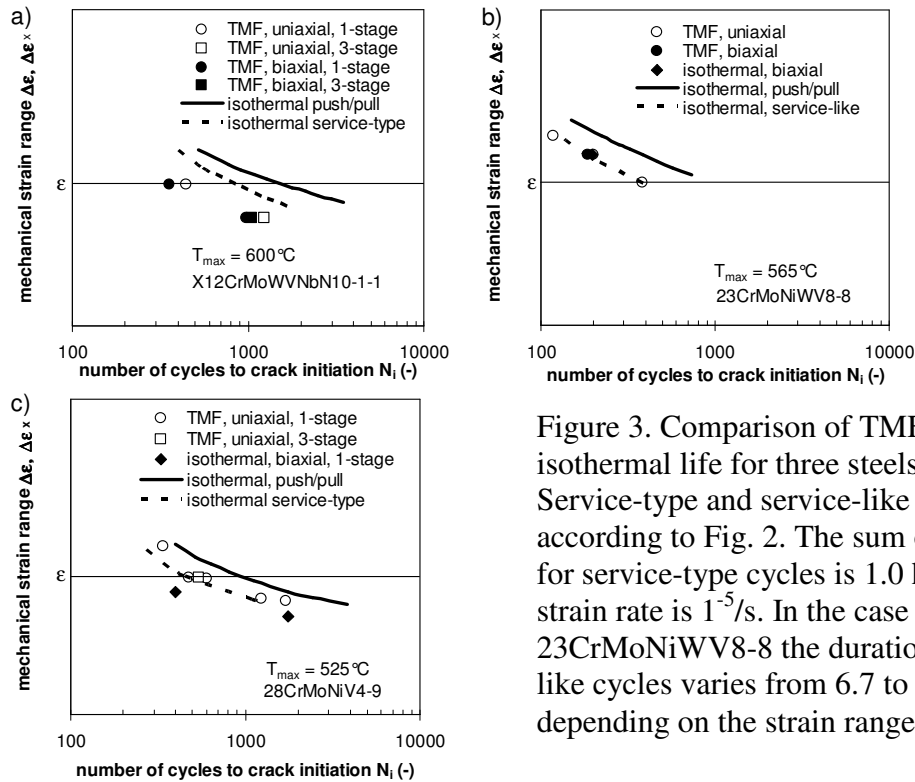


Figure 3. Comparison of TMF life and isothermal life for three steels (a), (b), (c). Service-type and service-like cycles are according to Fig. 2. The sum of hold times for service-type cycles is 1.0 h and the strain rate is $1^{-5}/\text{s}$. In the case of 23CrMoNiWV8-8 the duration of service-like cycles varies from 6.7 to 9.3h, depending on the strain range.

To study the influence of thermomechanical fatigue on lifetime, the ratio of N_i^{TMF} at TMF loading vs. N_i^{iso} at isothermal loading (the other experiment parameters are identical except temperature) has been evaluated [5]. Of interest is the observation that an increasing strain range corresponds to a smaller ratio of $N_i^{\text{TMF}} / N_i^{\text{iso}}$.

To study the influence of biaxial cruciform loading, the following observations have been made. At the steel X12CrMoWVNbN10-1-1 biaxial loading lead to a factor 1.3 shorter number of cycles to crack initiation N_i in comparison to uniaxial TMF. In the case of steel 23CrMoNiWV8-8 neither a decrease nor an increase of life values N_i were

observed. This is caused by the superimposed creep phases and the slow strain rate $<0.01\%/min$ at this specific cycle (Fig. 2b). Finally, at the steel 28CrMoNiV4-9 the influence of biaxial loading is smaller than factor 1.3. Summarizing, the basis for comparison of lifetime remains small. Therefore other methods e.g. the assessment of stress-strain-time-temperature hysteresis loops, the assessment of fatigue damage and creep damage according to the damage accumulation hypothesis or the recalculation of lifetime by the usage of a constitutive material model may help to achieve a better understanding of the influence of TMF-loading and multiaxial loading. This task is still ongoing. As a first observation from the stress-strain path analysis the stress relaxation behaviour of the modern steels is much more significant compared to the conventional 1Cr steel.

METALLOGRAPHIC EXAMINATION

The crack paths and damage distribution of the biaxial cruciform specimen under different loading conditions are shown in Fig. 4. On the specimen under push-pull loading at $300^{\circ}C$ (Fig. 4a), a main crack moves through the test zone. On the other specimens under isothermal loading at $600^{\circ}C$ and TMF loading with a maximum temperature of $600^{\circ}C$, the most damaged areas are located in the transition zone characterized by a transition radius. Here the cracks run along a direction which is at 45° to both axes (Fig. 4b, c, d). In the investigated isothermal biaxial tests, transgranular fatigue cracks can be observed. No microcracks can be found in the specimen at $300^{\circ}C$ (Fig. 5a). Beside the main crack, some microcracks starting from the surface are distributed over the entire test area in specimens under isothermal loading at $600^{\circ}C$ (Fig. 5b). The transgranular cracks, which are typical for fatigue dominant damage, initiate from the surface but sometimes also move along grain boundaries, representing intergranular cracking.

Considering the damage distribution at the termination of the TMF test (Fig. 5d), the most significant difference to isothermal biaxial tests (Fig. 5c) are separations, which occur predominantly perpendicular to the loading direction. Underneath the surface, separations are formed and distributed in the grains irregularly as well as on former austenite grain boundaries. Cracks which have initiated from the surface (Fig. 5d) connect with the matrix separations and move along a “zigzag” course, so that a crack network in conjunction with crack initiation from the surface leads to complex damage behavior. The observations made above are also confirmed in metallographic examinations of the 2%Cr steel on which complex biaxial isothermal loading as well as TMF loading were applied.

DISCUSSION

Systematic metallographic examinations show that microstructure damage observed on the isothermal specimens is fatigue dominated with superimposed creep damage (Fig. 4c). In contrast, damage on TMF specimens (Fig. 4d) are creep dominated due to the

matrix separation underneath the surface and fatigue dominated at the surface. FEA in [5] [7] on a uniaxial specimen showed that the local axial mean strain in the symmetry plane at axis is higher than that at the surface.

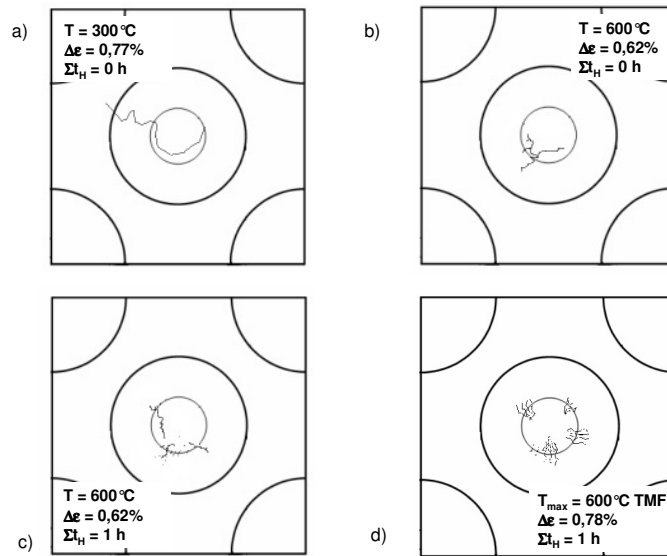


Figure 4. Crack path in cruciform specimens after push-pull experiment at 300°C (a), push-pull experiment at 600°C (b), three-stage service-type isothermal loading at 600°C (c) and single-stage TMF loading (d), schematically.

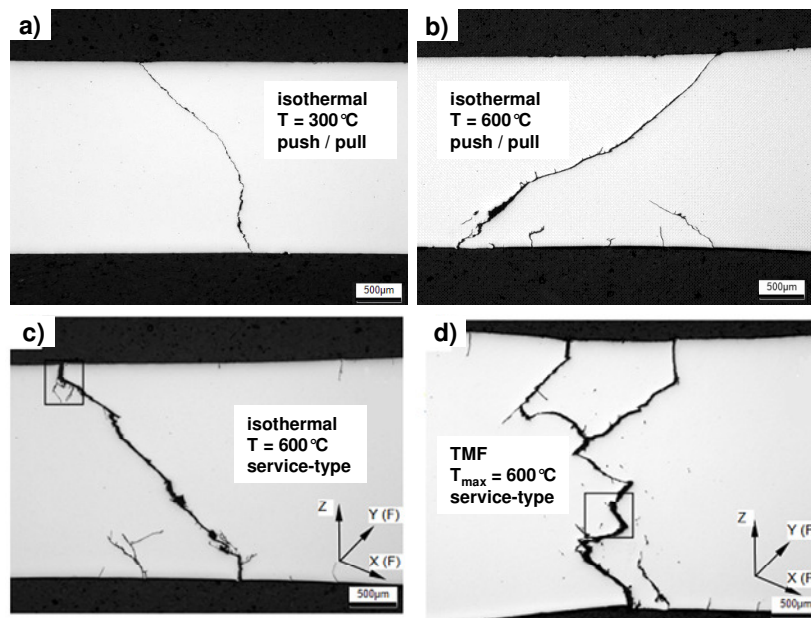


Figure 5. Crack path and microstructure of cruciform specimens after push-pull loading at 300°C (a), push-pull loading at 600°C (b), three-stage service-type isothermal loading (c), and single-stage TMF loading (d).

The significant separations observed in the matrix representing creep damage in these TMF specimens are assumed to exert the main influence on crack initiation at a reduced number of cycles [5] [7].

As a comparison, an FEA was conducted on the cruciform specimen under service-type TMF loading according to Fig. 5d. The applied constitutive material model implemented in user subroutine “UMAT” is of the type Chaboche [10]. An isotropic damage variable is incorporated in the model according to the principle of generalized energy equivalence [11]. Further, a user subroutine “UAMP” was developed to realize the so called “strain control mode”. The amplitudes of the strength F_x and F_y on the specimen arms are determined by UAMP and applied in every time increment of the FEA in order to reach the specified service-type cycle in the test zone.

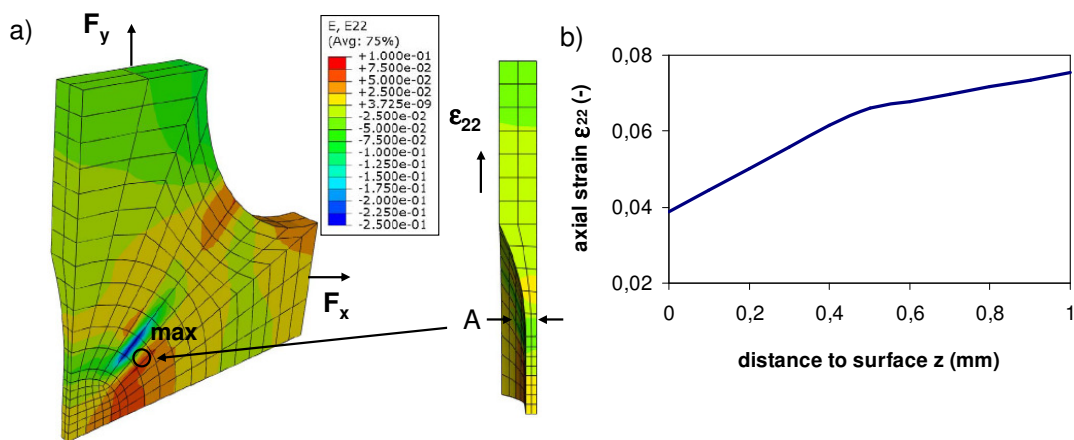


Figure 6. FEA calculated distribution of axial strain ϵ_{22} on cruciform specimen under biaxial TMF loading at end of life (a), cycle according to Fig. 2 a, b, and axial strain ϵ_{22} along the path A plotted against distance to the specimen surface (b).

An extrapolation method introduced in [8] was applied to reduce calculation time. As a result, a significant shift of axial strains (ϵ_{22}) is shown in the transition zone (Fig. 6a). An increasing local axial mean strain from the surface to symmetry plane can also be observed (Fig. 6b). This effect leads to the creep dominated damage and explains the building formation of separations, especially inside the specimen.

CONCLUDING REMARKS

A series of complex thermomechanical experiments partially with superimposed creep has been carried out on three rotor steels with varying chromium content using uniaxial specimens and cruciform specimens. The specimens under isothermal push-pull loading show typical fatigue damage: crack initiation from the surface and a transgranular cracking path. In the case of isothermal loading with hold time, fatigue cracks initiate from the surface which exhibit predominantly transgranular character but also move partly along grain boundaries. On the other hand, in the case of TMF loading with hold

time, separations caused by tensile strain ratcheting sub-surface lead to a “zigzag”-type crack path, representing transgranular, partly intergranular cracking. Service-type and service-like TMF tests lead to a lower number of cycles to crack initiation than isothermal loading. In comparison with creep fatigue results of heat-resistant steels with lower chromium content, modern heat-resistant steels lead to shorter TMF lifetime compared to isothermal lifetime under the same mechanical strain. Temperature rate plays an important role by the observed reduction of TMF lifetime. Finally biaxial loading of cruciform specimen causes a reduction of the number of cycles to crack initiation dependant on the type of steel.

Acknowledgements

Thanks are due to the „Forschungsvereinigung der Arbeitsgemeinschaft der Eisen und Metall verarbeitenden Industrie e.V.“ (AVIF No A232, A239) and the „FVV Forschungsvereinigung Verbrennungskraftmaschinen e.V.“ (FVV No 608 951, No 608 904) for financial support.

REFERENCES

1. Schwienheer, M., Haase, H., Scholz, A., Berger, C. (2002) in: Proceedings of the 7th Liège Conference on Materials for Advanced Power Engineering, Part III, 1409-1418, Lecomte-Beckers, J., Carton, M., Schubert, F., Ennis, F.J. (Ed.), Liège, Belgium.
2. Samir, A., Simon, A., Scholz, A., Berger, C. (2006) *Int. J. Fat.* **28** (5–6), 643-651.
3. Scholz, A., Berger, C. (2005) *Mat.-wiss.Werkstofftech* **36**(11), 722-730.
4. Reigl, M., Harish, N. D. (2007) in: Proc. of Eighth Int. Conf. on Creep and Fatigue at Elevated Temperatures, San Antonio, Texas
5. Cui, L., Wang, P., Hoche, H., Scholz, A., Berger, C. (2013) *Mater. Sci. Eng. A* **560**, 767-780
6. Zhang, S., Sakane, M. (2007) *Int. J. Fat.* **29**, 2191–2199.
7. Masserey, B. Colombo, F., Mazza, E., Holdsworth, S. (2003) *Fat. Fract. Eng. Mater. Struct.* **26** 1041-1052.
8. Wang, P., Cui, L., Scholz, A., Berger, C., Oechsner, M. (2012) *Int. J. Fat.* **440**, 253-259.
9. Simon, A., Scholz, A., Berger, C. (2009) in: Proceedings / Second International Conference on Material and Component Performance under Variable Amplitude Loading, Vol. 1, 505-516, DVM, Berlin.
10. Chaboche, J.L. (1989), *Int. J. Plast.* **5**, 247-302.
11. Tsakmakis, C., Reckwerth, D. (2003) In: Deformation and failure in metallic materials, pp. 381-406, Hutter, K., Baaser H. (Eds.), Springer, Berlin.
12. Simon, A., Scholz, A., Berger, C. (2007) *Mat.-wiss. u. Werkstofftech.* **38**, 8, 635-641.